UNIVERSITY OF AMSTERDAM

UvA-DARE (Digital Academic Repository)

The gamma Velorum binary system

De Marco, O.; Schmutz, W.; Crowther, P.A.; Hillier, D.J.; Dessart, L.; de Koter, A.; Schweickhardt, J.

Published in:
Astronomy & Astrophysics

Link to publication

Citation for published version (APA):
De Marco, O., Schmutz, W., Crowther, P. A., Hillier, D. J., Dessart, L., de Koter, A., & Schweickhardt, J. (2000). The gamma Velorum binary system. Astronomy & Astrophysics, 358, 187-200.

General rights
It is not permitted to download or to forward/distribute the text or part of it without the consent of the author(s) and/or copyright holder(s), other than for strictly personal, individual use, unless the work is under an open content license (like Creative Commons).

Disclaimer/Complaints regulations
If you believe that digital publication of certain material infringes any of your rights or (privacy) interests, please let the Library know, stating your reasons. In case of a legitimate complaint, the Library will make the material inaccessible and/or remove it from the website. Please Ask the Library: http://uba.uva.nl/en/contact, or a letter to: Library of the University of Amsterdam, Secretariat, Singel 425, 1012 WP Amsterdam, The Netherlands. You will be contacted as soon as possible.

UvA-DARE is a service provided by the library of the University of Amsterdam (http://dare.uva.nl)

Download date: 30 Apr 2017

Astron. Astrophys. 358, 187–200 (2000)

ASTRONOMY AND ASTROPHYSICS

The γ Velorum binary system*

II. WR stellar parameters and the photon loss mechanism

O. De Marco[1,2], W. Schmutz[3,2], P.A. Crowther[1], D.J. Hillier[4], L. Dessart[1,], A. de Koter[5], and J. Schweickhardt[6]**

[1] Department of Physics and Astronomy, University College London, Gower Street, London WC1E 6BT, UK
[2] Institut für Astronomie, ETH-Zentrum, Scheuchzerstrasse 7, 8092 Zürich, Switzerland
[3] PMOD/WRC, Dorfstrasse 33, Davos Dorf 7260, Switzerland
[4] Department of Physics and Astronomy, University of Pittsburgh, 3941 O'Hara Street, Pittsburgh PA 15260, USA
[5] Astronomical Institute Anton Pannekoek, University of Amsterdam, Kruislaan 403, 1098 SJ Amsterdam, The Netherlands
[6] Landessternwarte Heidelberg-Königstuhl, 69117 Heidelberg, Germany

Received 26 January 2000 / Accepted 28 March 2000

Abstract. In this paper we derive stellar parameters for the Wolf-Rayet star in the γ Velorum binary system (WR11), from a detailed non-LTE model of its optical and infrared spectra. Compared to the study of Schaerer et al., the parameters of the WC8 star are revised to a hotter effective temperature ($T_{\rm eff} \sim 57$ kK), a higher luminosity ($\log(L/{\rm L}_\odot)$ = 5.00), and a lower mass-loss rate (log($\dot{M}$ / M$_\odot$/yr) = -5.0, using a 10% clumping filling factor). These changes lead to a significant decrease in wind efficiency number, from 144 to 7, so that the driving mechanism of the wind of this WR star may be simply radiation pressure on lines. The derived spectroscopic luminosity is found to be 40% lower than that derived by De Marco & Schmutz through the mass-luminosity relationship for WR stars ($\log(L/{\rm L}_\odot)$ = 5.2).

The paper furthermore presents a comparison of the independently-developed modelling programs, CMFGEN and ISA-WIND. Overall, there seems to be very reasonable agreement between the derived parameters for WR11, except for the carbon content, which is 2 times higher for CMFGEN (C/He=0.15 vs. 0.06, by number). The comparison also confirms a disparity in the predicted flux at λ<400 Å, found by Crowther et al., which will have effects on several nebular line strengths.

The paper also presents the first independent check of the photon loss mechanism proposed by Schmutz. We conclude that, not only is it important to include very many lines to realistically model line blanketing, but in particular those ones that critically interact with strong resonance lines (e.g. He II λ303.78). The inclusion of these latter lines may significantly alter the wind ionization structure.

Key words: stars: atmospheres – stars: binaries: spectroscopic – stars: fundamental parameters – stars: individual: γ Velorum – stars: mass-loss – stars: Wolf-Rayet

1. Introduction

The double-lined spectroscopic binary γ Velorum (WC8 + O7.5) can be used to derive the mass of the Wolf-Rayet star, a quantity which cannot be directly determined in the case of single objects, but which provides an important constraint in computations of the late stages of massive star evolution. From it, and the mass-luminosity relationship for WR stars (Schaerer & Maeder 1992) a value for the WR luminosity can be derived and compared to that derived from spectroscopic analyses.

Orbital parameters together with the mass ratio were determined by Schmutz et al. (1997), while the 7.3σ HIPPARCOS distance allowed Schaerer et al. (1997) to derive the system's total mass ($\mathcal{M}$(O+WR)=29.5$\pm$15.9 M$_\odot$), the absolute visual magnitude (M_V(O+WR)=-5.39) and to carry out a preliminary spectroscopic analysis of both components. Schaerer et al. (1997), however, modelled only the WR He I λ4471 / He II λ4541 line strength ratio, *assuming* the mass-loss rate and the carbon abundance. Additionally, line blanketing was not accounted for by their model and their calculation used simple helium and carbon model atoms. Their stellar parameter determination should therefore be considered preliminary.

De Marco & Schmutz (1999; hereafter Paper I) carried out a full spectroscopic analysis of the O star through which its parameters were determined *simultaneously* with the light ratio between the WR and O stellar components. From a solution of the hydrodynamic wind equations, the mass of the O star was also derived and found to be consistent with the evolutionary O star mass. From it and the mass ratio of Schmutz et al. (1997), the mass of the WR star could be calculated (M$_\odot$=9.0$\pm$1.0 M$_\odot$). The combined mass of the system was therefore derived to be 39 M$_\odot$, higher than the value of Schaerer et al. (1997), but

* Based on observations collected at the European Southern Observatory at La Silla, Chile. ESO proposals Nrs. 56.D-327, 57.D-517 and 56.D-0700

** *Present address:* Département de Physique, Université Laval and Observatoire du Mont Mégantic, Quebec, QC G1K 7P4, Canada.
Correspondence to: od@star.ucl.ac.uk

consistent within their uncertainty. From the mass of the WR star and the theoretical mass-luminosity relation of Schaerer & Maeder (1992), a value for the WR bolometric luminosity was derived ($\log(L/L_\odot) = 5.2$), significantly higher than the spectroscopic luminosity derived by Schaerer et al. (1997; $\log(L/L_\odot) = 4.8$). Finally, using the synthetic O star spectrum, the WR11 spectrum was de-convolved from the O star component allowing the WR emission lines to be measured with greater accuracy.

In this paper we determine the stellar parameters of the WR star using the clumped, line-blanketed stellar atmosphere model CMFGEN (Hillier 1987, Hillier & Miller 1998). Ultimately, higher spectroscopic luminosities would lower the wind performance number, indicating that a smaller number of photon scatterings is needed to achieve the radiative driving of the wind. This would facilitate the derivation of the wind velocity law. γ Velorum provides us with a new tool to test the model luminosity with an independent method in such a way as to impose a further check on the wind momentun number.

A second aim of this paper is to continue the comparison of the non-LTE stellar atmosphere code CMFGEN and the independently developed Sobolev approximation code ISA-WIND (de Koter et al. 1993, 1997), which is used in combination with the line-blanketing Monte Carlo code of Schmutz (1991). This study follows from the comparison carried out by Crowther et al. (1999) for the WN8 star WR124.

Finally, Schmutz (1997) showed that line-line interaction between He II Lyα and metal lines at similar wavelengths can lead to a larger spectral luminosity. The inclusion of this interaction in the models, an effect that he called "photon loss", showed that WR6 might have a larger luminosity than previously thought, and allowed him to calculate a velocity law for its outer wind. Since line-line interaction is included in the CMFGEN model code, we can test whether the approximation of Schmutz (1997) is valid and quantify the importance of the photon loss effect in the case of WR11.

In Sect. 2 we summarise the observations, while in Sect. 3 we discuss the light ratio between the O and WR stars and the reddening towards the system. In Sect. 4 we describe the model atmosphere codes used in the determination of the stellar parameters. We present our results in Sect. 5, together with the code comparison, while in Sect. 6 the effect of photon loss is studied. We finally draw our conclusions in Sect. 7.

2. Observations and reduction

Our optical observations of γ Velorum are the same as those used by Schmutz et al. (1997), where a full account of the data reduction can be found. In summary, several spectra have been obtained at the 50 cm ESO telescope in conjunction with the Heidelberg Extended Range Optical Spectrograph (HEROS) in the ranges 3500–5500 Å and 5800–8600 Å covering the binary period. The resolution is R=20 000, while the S/N ratio ranges between 100 at 3600 Å and 250 at 6000 Å. The phase-averaged spectrum of the γ Velorum system was rectified as described in Paper I. It is important to remind that rectification of WC stars is a very delicate operation because of blending of large numbers of broad lines, which leave few identifiable continuum points. Moreover, spectral ranges at the end of instrumental orders (5300–5500 Å and 5800–5900 Å), suffer from additional uncertainty. Unfortunately this affects the diagnostic lines He I λ5876, He II λ5412, and C IV λ5471. Extreme care was taken in rectifying these ranges and consistency between these lines and those residing at other wavelengths was insured.

Observations of the 10830 Å He I line were obtained at the European Southern Observatory (ESO) New Technology Telescope on January 12 and 13, 1996, with the EMMI instrument. EMMI was used in the REMD mode with grating No. 7, a slit-width of 1.5$''$ and the spectrum recorded on ESO CCD No. 36. Two exposures, each lasting 10 s, were taken. Wavelength calibration was obtained with respect to a ThAr arc lamp, to achieve a resolution of 2 Å. Relative flux calibration was obtained with respect to a 180 s exposure of the standard star θ Crt.

Mid-IR data of WR11 were obtained as part of Guest Observer programme WRSTARS (P.I. van der Hucht), with the Short Wavelength Spectrograph (SWS; de Graauw et al. 1996) on board the ESA Infrared Space Observatory (ISO; Kessler et al. 1996). The SWS AOT6 observing mode was used to achieve full grating resolution, $\lambda/\Delta\lambda \sim 1300$–$2500$, with the wavelength coverage 2.38–45.0 μm. The observations were flux calibrated to an accuracy of 5% and $\sim$20% for the low and high wavelength ends, respectively. The possibility that the nearby γ^1 Velorum might have contaminated the ISO observations of γ Velorum was investigated, but with an aperture of 20$''$ centered on γ Velorum it is not possible that light from γ^1 Velorum, at 40$''$ distance, could have entered the aperture. For full details on the observations and data reduction procedures, we refer the reader to Morris et al. (2000).

Finally, we have obtained a flux-calibrated UV dataset for WR11 as follows. WR11 was too bright for absolutely flux calibrated observations with IUE/LORES. Consequently we have matched IUE observations from July 1988, to low resolution S2-68 observations from 1973 at phase 0.3 (Willis & Wilson 1976).

3. Light ratio correction and reddening

In this section we discuss the O-WR light ratio of γ Velorum. We also re-evaluate the interstellar reddening that was adopted in Paper I, namely $E(b-v) = 0.03$ mag, obtained from assumed intrinsic colours (van der Hucht et al. 1988).

The spectrum of γ Velorum used here is the same phase-averaged rectified spectrum used in Paper I. Correction for the continuum as well as the line contribution of the O star was carried out in that paper using the model O star spectrum and the deduced value of the light ratio. A light ratio of L(O) / L(O+WR) = 0.795 $\pm$0.020 was obtained in Paper I from an average of three lines, namely He I λ4471, He I λ4922 and He II λ4541. Assuming that this light ratio is representative for this spectral range, we derive the wavelength dependence of the light ratio using synthetic spectra for the O star from Paper I, and for the WR star from the following section. The ratio of these continuum distributions, adjusted such that L_λ(O) / L_λ(WR)

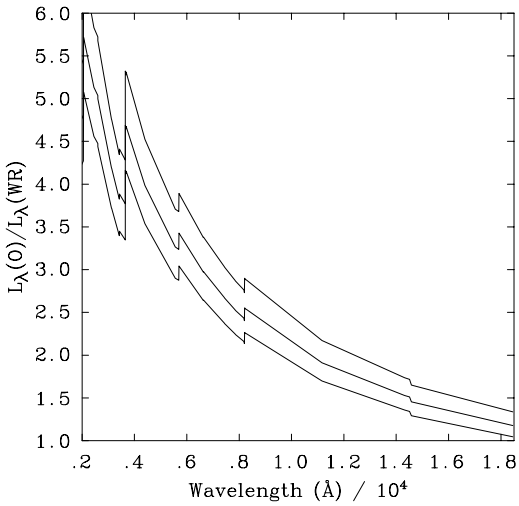

Fig. 1. The light ratio, L_λ(O)/L_λ(WR), as a function of wavelength. The upper and lower lines show the error bars derived from the original error limits of Paper I

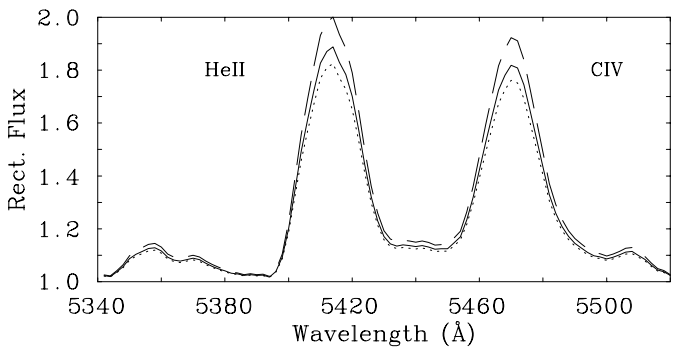

Fig. 2. Effect of the light ratio uncertainty on the strength of important diagnostic lines at He II λ5412 and C IV λ5471. (This does not include errors on the synthetic atmospheres used in the construction of the wavelength-dependent ratio). The dashed and dotted curves correspond to the upper and lower error bars, respectively

= $3.88^{+0.5}_{-0.4}$ at λ= 4700 Å, is plotted in Fig. 1, together with error bars. A calibration curve L_λ(O+WR) / L_λ(WR) is created and applied to the optical spectrum of WR11 to account for the contribution of the O star continuum to the WR equivalent widths. In Fig. 2 we show the effect that the error bars from the light ratio have on He II λ5412 and C IV λ5471.

After the spectrum is rectified and light-ratio corrected, a model can be calculated to fit the WR lines, as discussed in the following section. First, we preempt the result of this modelling in order to verify our choice of reddening. Published broad-band Johnson V magnitudes for γ Velorum span a wide range, from V = 1.70 (Cousins 1972) to V = 1.83 (Johnson et al. 1966). We suspect that the broad band observations suffer from contaminations by nearby spectral lines such as C IV λ5806 and that the measured brightness depends crucially on the exact sensitivity curve of the used setup. Therefore, in order to minimise the contamination of WR line emission, we prefer to adopt the narrow-band ubv Smith (1968) photometry. Following the corrections by Schmutz & Vacca (1991) to the Smith datasets, we obtain $v = 1.70$ mag and $b - v = -0.32$ mag. Our theoretical combined O+WR model reveals $(b - v)_0 = -0.33$ mag, implying $E(b - v) = 0.01$ or $E(B - V)$ = 0.01 mag.

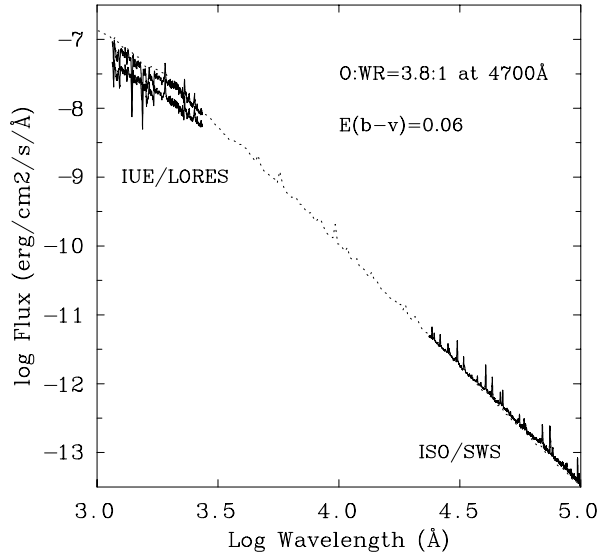

Fig. 3. Comparison of the combined O+WR synthetic model (dotted line) and the IUE/LORES and ISO/SWS observations (solid lines) for reddenings of $E(b - v)$ = 0.00 and 0.06 mag, with a light ratio $L_{\lambda 4700}$(O)/$L_{\lambda 4700}$(WR) = 3.8

We have also carried out an alternative reddening determination, by fitting the combined WR+O model to UV (IUE/LORES) and IR (ISO) spectrophotometry, de-reddened following Seaton (1979). Fig. 3 compares observed and de-reddened spectrophotometry (solid lines) with theoretical models (dotted lines), revealing $E(b - v) = 0.06$ or $E(B - V)$ = 0.07 mag. Unfortunately, we are unable to reconcile these discrepant reddening values, and so adopt $E(b - v) = 0.035$ mag ($E(B - V)$ = 0.04), in good agreement with van der Hucht et al. (1988). Note that for this reddening and the adopted light ratio, the combined O+WR model flux lies ∼10% higher than the UV IUE observed fluxes and a similar value below the IR ISO observations.

The distance modulus of 7.06 mag (corresponding to a distance of $[258^{+41}_{-31}]$ pc, HIPPARCOS[1] and de-reddened v = 1.56 mag imply M_v(O+WR) = -5.50. The O/WR continuum light ratio is 3.61 at the v-band (Fig. 1) so that M_v(O)=–5.23 and M_v(WR) = –3.84. We may convert the Smith (1968) v to Johnson V via $V = v - 0.365(b - v) + 0.007$, adapted from Turner (1982) to take account of the ubv re-calibration by Schmutz

[1] The HIPPARCOS distance to γVelorum has been recently put in doubt (Pozzo et al. 2000) by the finding of a new population of pre-main sequence stars which might be associated with the binary. This new value of the distance re-positions γ Velorum within the Vela OB2 association at a distance of 360–490 pc, in agreement with earlier estimates. Clearly, adopting a larger distance would have a dramatic effect on distance dependent parameters, such as luminosity, radius and mass-loss (for a distance of 360–490 pc, $\Delta \log(L/\mathrm{L}_\odot)$=0.3–0.6). We have, however, maintained the 7.3σ HIPPARCOS distance measurement, which we trust to be the best distance estimate to date.

& Vacca (1991). From theoretical continuum O and WR distributions we obtain $(b-v) = -0.34$ and $(b-v) = -0.20$, respectively, revealing absolute line free V-magnitudes listed in Table 1. Relative to Paper I, the difference in the absolute magnitude of the O star, M_V(O), is -0.04 magnitude. The errors listed in Table 1 are solely from the reddening and light ratio uncertainties. Errors in the distance, would add an additional 0.3 mag in the M_V uncertainties. Propagating these errors onto the derived magnitudes and luminosities in Table 1, and subsequently onto the spectroscopic properties in Sect. 5, introduces an additional systematic error of $\log\ (L/L_\odot)$=±0.1 for both cases. In this way we lose sight of the actual accuracy reached by this study.

To be consistent with the slight change in the O and WR star V magnitudes we have revised the uncertainties on L, $\mathcal{M}$ and i, while the values of the luminosity and mass of the WR star are also slightly modified.

Table 1. O and WR and system parameters, updated from Paper I. From these the mass and luminosity of the WR star are determined. Errors on the distance are not taken into account – see text

$\Delta M_{\lambda 4700}$	1.47± 0.13 mag
$f_{\lambda 4700}$(O)/$f_{\lambda 4700}$(O+WR)	0.795 ± 0.020
M_V(O+WR)	–5.5 ± 0.3 mag
i	63±3 deg
M_V(O)	–5.10 ± 0.1 mag
$T_{\rm eff}$(O)	35 000±300 K
N[He](O)	0.087 (by number)
R(O)	12.4±1.7 $R_\odot$
L(O)	(2.1±0.3)×10^5 $L_\odot$
$\mathcal{M}$(O)	30±2 $M_\odot$
$\dot{M}$(O)	(1.78±0.37)×10^{-7} $M_\odot yr^{-1}$
v_∞(O)	2500±250 km s^{-1}
age(O)	(3.59±0.16)×10^6 yr
M_V(WR)	–3.76 ± 0.2 mag
$\mathcal{M}$(WR)	9.5±1.0 $M_\odot$
L(WR)	(1.7±0.4)×10^5 $L_\odot$

4. Stellar atmosphere codes

In this section we present a summary of the description of both codes used (a full account can be found in Hillier, 1989 and Hillier & Miller, 1998 for CMFGEN and in de Koter et al., 1993, 1997, for ISA-WIND). Along with the description of the basic codes, we give an account of the Monte Carlo line blanketing code used in conjunction with the un-blanketed ISA-WIND to calculate the additional opacity due to the effect of bound-bound transitions on the continuum photons. Last, the implementation of the photon loss mechanism (Schmutz 1997) into the Sobolev code is presented here, for the first time, and a parallel is drawn with the potential effect of line-line interaction in the line-blanketed code CMFGEN.

4.1. CMFGEN

CMFGEN (Hillier 1987, 1990; Hillier & Miller 1998, 1999) solves the transfer equation in the co-moving frame, subject to statistical and radiative equilibrium, assuming an expanding, spherically-symmetric, homogeneous or clumped, time-independent atmosphere. Line blanketing is treated correctly in the transfer problem, except that a simplifying 'super level' approach is used (Anderson 1989), by which several levels of similar energies and properties are treated as a single 'super level'. The population of an individual atomic level in the full model atom is determined by assuming that it has the same departure coefficient as the corresponding super level to which it belongs. For the specific models dealt with in this paper the atomic model is shown in Table 2. Elemental abundances other than hydrogen, helium, carbon and oxygen, are fixed at their solar mass fraction values.

The stellar radius (R_*) is defined as the inner boundary of the model atmosphere and is located at Rosseland optical depth of ∼20 with the stellar temperature (T_*) defined by the usual Stefan-Boltzmann relation. Similarly, the effective temperature ($T_{\rm eff}$) relates to the radius ($R_{2/3}$) at which the Rosseland optical depth equals 2/3. There is now overwhelming evidence for the clumped nature of WR stars (e.g. Moffat 1999), so we have adopted a simple filling factor approach. Following the method proposed by Schmutz (1995), we assume that the wind is clumped with a volume filling factor, f, and that there is no inter clump material. Since radiation instabilities are not expected to be important in the inner wind we parametrise the filling factor so that it approaches unity at small velocities. Clumped and non-clumped spectra are very similar, except that line profiles are slightly narrower with weaker electron scattering wings in the former. Although non-clumped models can be easily rejected, we are unable to determine the clumping factor because of the severe line blending in WC winds. We can therefore derive only $\dot{M}/\sqrt{f}$ with our spectroscopic analysis.

Unfortunately, individual line blanketed co-moving frame calculations are generally computationally demanding, despite the use of super levels, so that a large parameter space cannot be quickly explored. One solution is to (i) solve the transfer problem in the classical Sobolev approximation rather than the co-moving frame, which the code ISA-WIND does (de Koter et al. 1993, 1997), and (ii) consider line blanketing via Monte Carlo sampling following Schmutz (1991, 1997) allowing the opacity of a huge number of lines to be considered.

4.2. ISA-WIND *and the Monte Carlo line-blanketing code*

The improved Sobolev approximation code (ISA-WIND) is described in detail by de Koter et al. (1993, 1997). The principal differences with CMFGEN relate to (a) the treatment of the line radiation transfer; (b) wind electron temperature which assumes a grey atmosphere in local thermodynamic equilibrium (LTE); (c) the specific atomic model treated, as listed in Table 2.

The co-moving frame method consistently treats a possible change of properties of the medium inside the region in which line photons can be absorbed and re-emitted. In the Sobolev approximation one assumes this line interaction region is infinitely

small. More exactly, the Sobolev approximation assumes that the source function and the opacities are linear functions such that they can be taken out of the transfer integral. This is generally a valid assumption for Wolf-Rayet stars, where the large velocity gradient of the flow results in a small interaction zone. The Sobolev classical approximation (Castor 1970) implies that interactions of line photons with the continuum inside of the (in reality extended) interaction region are ignored. However, the improved Sobolev approximation code ISA-WIND does include such continuum interactions. Note that use of the Sobolev approximation introduces great simplifications in the radiative transfer, resulting in an overall iteration process up to about 20 times faster compared to the co-moving frame approach.

Turning to line blanketing, an iterative technique including the Monte Carlo method of Schmutz (1991) is employed. The method allows the computation of intensity-weighed effective opacity factors, which account for the presence of tens of thousands of spectral lines, dominated by Fe and Ni. Based on ISA-WIND atmosphere calculations, the Monte Carlo code determines the line blanketing factors. An iterative procedure is used, such that blanketing factors are used by the non-LTE code to calculate a new atmosphere, which in turn is used to calculate new blanketing factors. A few iterations are generally sufficient. This is due to the fact that the scattering and absorption factors are not very sensitive to the exact model intensity.

The Monte Carlo method deals with the photon scattering in the correct manner, although no branching is taken into consideration, an effect that would tend to re-distribute UV photons to longer wavelengths. The ionization equilibrium of metal species is also approximate, in that it is determined in relation to the non-LTE structure of helium, carbon and oxygen and not by the full solution of the statistical equilibrium equations for those species.

4.3. Photon loss

"Photon loss" is the name given by Schmutz (1997) to the interaction between the photon field of the He II Lyα line at 303.78 Å and nearby metal lines (e.g. the O III Bowen lines at 305.72 and 303.65 Å). This was suggested by Schmutz (1997) to be responsible for a decrease in the ionization equilibrium of the wind of WR6 (WN4), with respect to the equilibrium obtained when no such line-line interaction was accounted for. In order to fit the observed spectrum when photon loss is included in the model, the model's stellar temperature has to be higher, which results in a higher spectroscopic luminosity. This contributes to a lower wind performance number and allowed Schmutz (1997) to calculate a velocity structure for the outer wind of WR6.

Since line-line interaction was not accounted for in any atmospheric wind code before Hillier & Miller (1998) implemented it into the Hillier (1990) code, Schmutz (1997) calculated the photon loss factor (i.e. the amount of interaction between the He II Lyα and nearby metal lines) by comparing the opacity of metal lines in the 303-Å region to that of the He II Lyα line (his Appendix A). Once the amount of interaction is known for a particular model atmosphere, a corresponding fraction of photons can be taken out of the radiation field at that particular wavelength for all grid points. In this way the same fraction of photons is removed from the radiation field at all depth points, although in reality the photon loss factor depends on the relative opacity of the He II Lyα line and that of the metal lines, which in turn depends on the depth-dependent populations. This problem however is not critical as long as the opacity of metal lines behaves similarly to that of helium. Additionally, the loss of photons is only critical for the point in the atmosphere where the wind is recombining. We implemented the photon loss approximation into the ISA-WIND code of de Koter et al. (1993 – see Sect. 4.3.1) and used it in the calculation of a model for WR11.

CMFGEN includes line-line interaction and as such it should naturally include the photon loss effect, provided the specific metal lines in the He II Lyα region are included in the model atom. We can therefore test whether this effect and its consequences for the stellar luminosity has been accounted for properly by our approximation.

4.3.1. Implementation of photon loss in ISA-WIND

Once the photon loss factor, f, is calculated for a certain model atmosphere (see Schmutz 1997, Appendix A), a fraction f of the photons is removed from the radiation field in the wavelength range 300–304 Å. To do so, one has to modify the expression where the mean intensity for this line wavelength is calculated at every code iteration. In ISA-WIND this was achieved via a modification of the Sobolev escape probability.

In the Sobolev approximation the radiation field $\bar{J}$ at radius point r is related to the line source function S in the following way:

$$\bar{J}(r) = (1-\beta)S(r) \tag{1}$$

where β is the line escape probability by direct flight and where

$$S(r) = \frac{N_u A_{ul}}{N_l B_{ul} - N_u B_{ul}} \tag{2}$$

with N_u and N_l the upper and lower level populations, respectively, A_{ul} and B_{ul} the Einstein coefficients. Due to photon loss, the field at frequencies close to the He II Lyα is modified in the following way:

$$\bar{J}(r) \rightarrow (1-f)\bar{J}(r). \tag{3}$$

Substituting (1) into (3) we obtain:

$$\bar{J}(r) = (1-\beta-f+f\beta)S(r) \tag{4}$$

Comparing (4) to (1) we see that the classical Sobolev escape probability is modified in the following way:

$$\beta \rightarrow (\beta + f - f\beta).$$

5. Stellar analysis

In this section we present the stellar parameters for WR11 derived with the two codes CMFGEN and ISA-WIND (supplemented

Table 2. Summary of model atom used in CMFGEN and ISA-WIND radiative transfer calculations, including full levels ($N_{\rm F}$), super levels ($N_{\rm S}$) and total number of transitions ($N_{\rm Trans}$), following Hillier & Miller (1998) and de Koter et al. (1997; 31 auto-ionizing levels are included for C III in the atomic data used by ISA-WIND)

Ion	$N_{\rm S}$	$N_{\rm F}$		$N_{\rm Trans}$		Details	
	CMFGEN	CMFGEN	ISA-wind	CMFGEN	ISA-wind	CMFGEN	ISA-wind
He I	27	39	51	905	588	$n \leq$14	$n \leq$20
He II	13	30	20	435	190	$n \leq$30.	$n \leq$20
C II	39	88	7	791	10	$nl \leq$2s2p3p^{2}D	$nl \leq$2s^2(^{1}S)3d^{2}D
C III	99	243	44	5513	174	$nl \leq$2s10z^{1}Z	$nl \leq$2s(^{2}S)5f^{1}F$^\circ$
C IV	49	64	15	1446	105	$n \leq$30	$n \leq$10
O II	23	75	–	3	–	$nl \leq$2p$^{3\,2}$P^o	–
O III	50	50	3	213	–	$nl \leq$2p3d^{1}D^o	2s^{2}2p^2(^{1}S)
O IV	30	72	22	67	52	$nl \leq$2s2p4d^{2}P^o	2s2p(^{3}P$^\circ$)3d^{4}D
O V	31	91	24	835	57	$nl \leq$2s4f^{1}F^o	2p(^{2}P)3p^{1}S
O VI	13	19	26	749	153	$nl \leq$8d^{2}D	1s^2(^{1}S)10d^{2}D
Si IV	12	20	–	72	–	$n \leq 20$	–
Ca III	16	39	–	104	–	$nl \leq$3s^{2}3p^{5}5s^{3}P^o	–
Ca IV	8	26	–	12	–	$nl \leq$3s^{2}3p^4(^{1}D)3d^{2}D	–
Ca V	19	32	–	44	–	$nl \leq$3s3p^4(^{4}P)3d^{5}D	–
Ca VI	16	30	–	61	–	$nl \leq$3s3p^3(^{3}D)3d^{4}G^o	–
Fe IV	21	280	–	3767	–	$nl \leq$3d^4(^{1}G^o)4p^{2}P^o	–
Fe V	19	182	–	1921	–	$nl \leq$3d^3(^{2}D^o)4p^{1}P^o	–
Fe VI	10	80	–	617	–	$nl \leq$3d^2(^{1}S)4p^{2}P^o	–

by the Monte Carlo line-blanketing code). We will discuss the quality of the fits and the overall flux distribution of the model atmospheres.

5.1. Analysis technique

In our approach, diagnostic optical lines of He I ($\lambda\lambda$5876, 10830) and He II ($\lambda\lambda$4686,5412) are chosen to derive the stellar temperature and mass-loss rate. Initially we assume the carbon and oxygen abundances to be the same as those derived for the single WC8 star WR135 by Dessart et al. (2000), because of the similarity of the two spectra (a comparison of the rectified spectra is shown in Fig. 5). Once a fair agreement is reached between the modelled and the observed helium lines, carbon and oxygen abundances can be altered to improve the fits to their diagnostic lines. For carbon, lines of C III at 6741 Å and of C IV at 5471 Å are used. For oxygen, the lack of good diagnostic lines in our spectral range and the weak and blended nature of those that can be identified, make the determination of the oxygen abundance impossible. We therefore adopt the theoretical O/C number ratio of 0.2 (Meynet et al. 1994). Changing oxygen and carbon abundances acts on the total opacity of the wind and therefore feeds back on the modelled strengths of the helium lines. Parameters have therefore to be adjusted so as to retrieve the fits of the helium lines.

We adopt the wind terminal velocity determined by St.Louis et al. (1993), $v_\infty = 1550$ km s^{-1}, from the variability of the UV spectrum. The velocity law used by the CMFGEN code (Hillier & Miller 1999) is a two component "beta" law which produces a slower flow than the usual β = 1 velocity law, at points in the atmosphere intermediate between the outer regions where $v \rightarrow v_\infty$ and the photosphere. Hillier & Miller (1999) found that it leads to better fits to the line profiles, while at the same time Schmutz (1997) determined a similar velocity law from his hydrodynamic calculation (which, however was carried out only for the outer layers of the wind). The two component velocity law used for our calculations uses v_0 = 100 km s^{-1} (the photospheric velocity), $v_{\rm core}$ = 1.0 km s^{-1} (the velocity at R_*), $v_{\rm ext}$ = 1100 km s^{-1} (the intermediate velocity) and v_∞ = 1550 km s^{-1} (the terminal velocity). The two beta exponents used are 1.0 and 50, for β_1 and β_2, respectively. The ISA-WIND calculation was performed with the same velocity law as CMFGEN. A clumping filling factor of 0.1 was adopted for CMFGEN. Usually this is derived together with the other parameters, by fitting line wings; for WC stars the heavy blending makes this task harder. We therefore adopted the value obtained by Hillier & Miller (1999) and confirmed by Dessart et al. (2000).

The atomic data models used for the two codes are summarised in Table 2 (see Dessart et al. (2000) for a description of the atomic data used in CMFGEN, while ISA-WIND uses the latest Opacity Project data). Note that the number of individual and super levels (N_F and N_S) mean different things for the two codes: CMFGEN bundles N_F levels into N_S super-levels, while all ISA-WIND atomic levels, listed under the N_F heading, are treated individually (apart for He I and C IV for which the upper 32 and 6 levels, respectively, are super-levels). The data used by CMFGEN is more extensive than those used by ISA-WIND. Generally this can have an effect on the ionization equilibrium (and hence on the spectrum), or only have an effect on particular lines between high lying levels. Tests using CMFGEN with reduced atomic data show that while individual lines can be very sensitive to the amount of levels used (e.g. C III λ8500) the

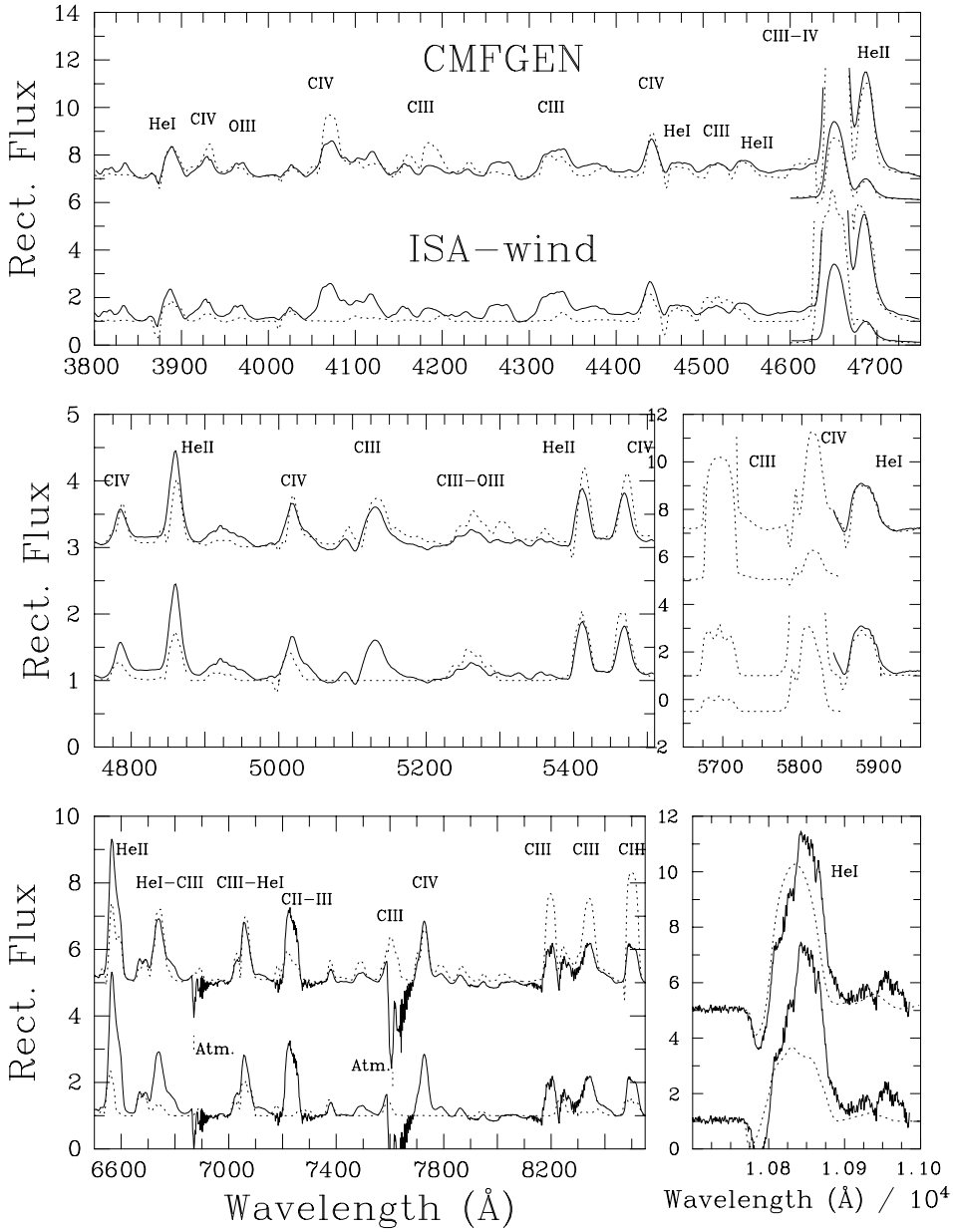

Fig. 4. Comparison between the rectified optical (HEROS) spectrum of WR11 (solid line) with the synthetic spectrum produced by CMFGEN (upper spectrum, dotted line) and ISA-WIND (accounting for line blanketing – lower spectrum, dotted line). For clarity of display, the regions 4600–4700 Å and 5650–5850 Å are multiplied by 0.2 and 0.3, respectively, and offset

overall ionization of the wind is not critically dependent on the size of the atomic model provided a minimum amount of levels is used.

5.2. Optical and infrared line fits

The overall fit quality of the helium diagnostic lines is fair and comparable for the two codes (Fig. 4). Due to the difficulties in rectifying WC spectra and the weakness of the lines in the region 4400–5450 Å region, it was decided that the He I $\lambda\lambda$5876,10830 would be better diagnostic lines than He I λ4471, although the fit to this line is not inconsistent. λ5876 is very well reproduced by CMFGEN, while λ10830 is under-predicted by about 15% (one should take into account that this line was not corrected for the O star absorption line, which can be observed as a depression on its blue side). ISA-WIND only reproduces λ5876 (albeit not perfectly), due to the sensitivity of λ10830 to the outer wind electron temperature, which is calculated in the grey LTE approximation and fixed for outer radii to 10 000 K.

He II λ5412 is well reproduced by both codes, although CMFGEN slightly over-predicts it. Once again we use the 4440–4600 Å region only as a secondary diagnostic: CMFGEN does reproduce the He II λ4541-C IV λ4553 rather well, while ISA-WIND does not predict the C IV component in the blend with an overall poorer result. λ4686 is slightly under-predicted by CMFGEN, with the ISA-WIND synthetic line fit being affected by blending with the over-predicted C III-C IV line at 4660 Å.

The He II lines at λ4859 and λ6560 Å are underestimated by both CMFGEN and ISA-WIND, by about 20% and 80% respectively. In the case of λ6560 the presence of an under-predicted flat-topped C II line could be responsible (see below). It is in fact

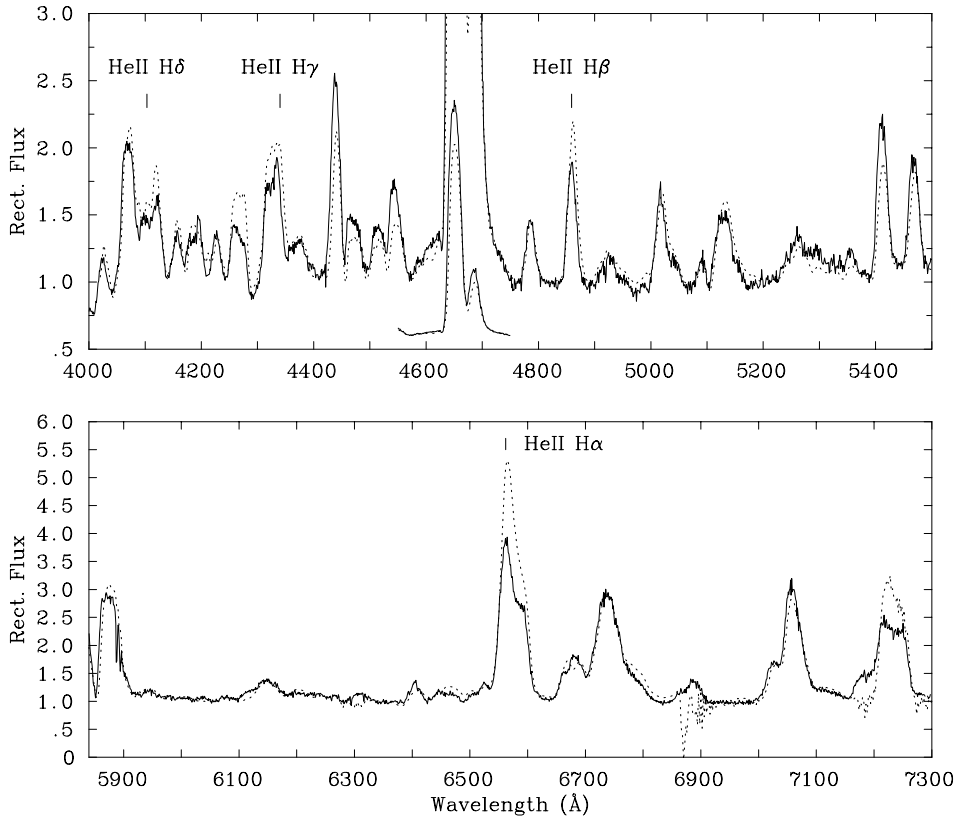

Fig. 5. Comparison between WR135 (solid line) and WR11 (dotted line), showing the similarity of the two spectra except for the He II lines at 4859 and 6560 Å

not uncommon that models under-predict line emission from low ionization stages (cf. C IIλ4267), showing that the stratification of the wind is imperfectly reproduced. It is possible that this problem will be solved once more realistic clumping is included in the models. On the other hand there is no blend in λ4859 that could be blamed for the poor fit. For that line there could be a slight rectification problem, although this alone could not account for the amount by which the model under-fits the data.

In Fig. 5 we show a comparison of the observed spectra of WR11 and WR135. The two spectra are very similar with WR135 having only slightly stronger He II $\lambda\lambda$4541, 4686, 5412 lines and comparable He I $\lambda\lambda$5876,7066 lines. On the other hand, WR11 has stronger He II $\lambda\lambda$4339, 4859, 6560, indicating an opposite trend to the rest of the He II spectrum! (He II λ4100 is also shown in Fig. 5 although due to the heavy blending with carbon lines, it is difficult to make a clear comparison). This points to an anomaly in the strength of these He II Pickering lines. We should also note that the ratio of He II5411 to Hβ is different for the two stars, indicating something anomalous in the line formation in one or both stars.

For carbon lines, CMFGEN reproduces strengths and shapes to a higher degree of accuracy. ISA-WIND synthetic lines underestimate C IV $\lambda\lambda$4440,4780 by about 20% and 40%, respectively, while C III $\lambda\lambda$6741,8500 are weaker than the observations by 80% and 50%, respectively. On the other hand while CMFGEN reproduces $\lambda\lambda$4440,4780,6741, the C III line at 8500 Å is over-estimated by more than 100%. The λ4660 C III - C IV blend is overestimated by ISA-WIND ($\sim$60%), while it is underestimated by CMFGEN ($\sim$10%). Some lines of C III (e.g. $\lambda\lambda$8196,8500) and C IV (λ7063), are under-predicted or not predicted at all by ISA-WIND partly because they are not accounted for in the atomic model. The carbon abundance determination, however, rests critically on the ratio of He II λ5412 / C IV λ5471 which is well matched by both codes. C II is under-predicted by CMFGEN and not predicted at all by ISA-WIND (which includes only 7 levels in the atomic model of C II). However the presence of the C II line at 4267 Å indicates that C II lines are present in the spectrum. The spectral classification lines C III λ5696 and C IV λ5806 are not included in the observations, so in Fig. 4 we only show the prediction for both models. These two lines are remarkably different in the two models: the spectral types deduced from their equivalent width ratio are WC6 and WC9 for the ISA-WIND and CMFGEN codes, respectively, where the criteria of Crowther et al. (1998) have been adopted. The model for WR135 of Dessart et al. (2000), with similar parameters, has a much larger C IV λ5806/C III λ5696 line ratio, consistent with a WC8 classification. Although these two lines form an excellent spectral type diagnostic because of their mutual proximity and their strengths, it is important to note that the correspondence of their strengths to the stellar parameters is not straight forward.

Differences in the carbon spectrum are obtained (De Marco et al. 1999b) not only between CMFGEN and ISA-WIND, but also with the co-moving frame code of Koesterke & Hamann (1995). Such discrepancies are not due to differences in the atomic data, and it is extremely difficult to identify the exact cause, since the effect is highly dependent on the parameter space investigated. Further investigations are under-way.

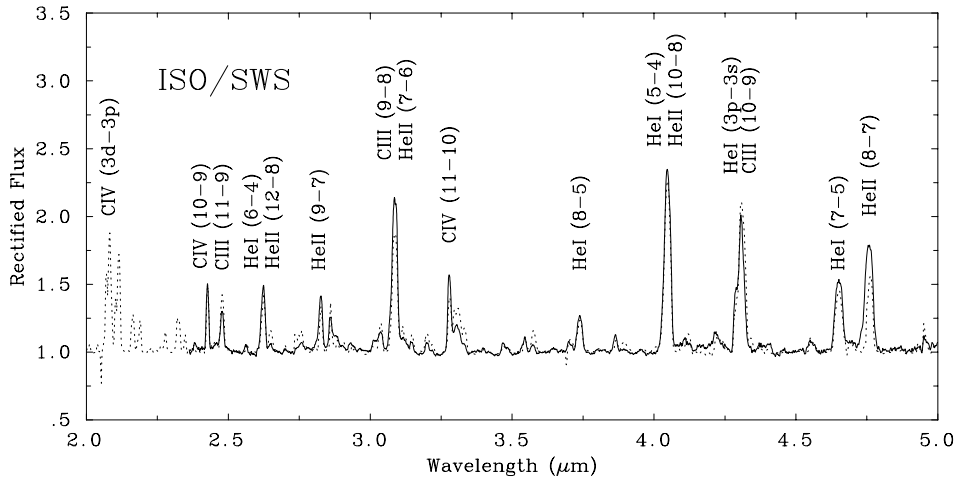

Fig. 6. Comparison of the rectified ISO observations of γ Velorum (solid) with the CMFGEN model (dotted) scaled to the optical $L_{\lambda 4700}$(O) / $L_{\lambda 4700}$(WR) = 3.8

A comparison of the CMFGEN synthetic spectrum with the rectified ISO spectrum of γ Velorum is shown in Fig. 6. Our WR+O model spectrum fits the emission lines to a good level of accuracy, demonstrating that line fits are consistent also in the IR. Spectral features in the H and K windows agree qualitatively with unpublished AAT spectroscopy of L.F. Smith (priv. com.). As mentioned in Sect. 3, the combined O+WR model continuum is ∼10% lower than the flux-calibrated ISO spectrum for the adopted light ratio, reddening and observed v magnitude.

In conclusion it was felt that given the limitations of the observed spectra, the parameters of WR11 from the optical fits have been constrained rather well. The uncertainties listed in Table 3 are determined from the fits (for the T_*, $\dot{M}$, C/O and v_∞ parameters) or from error propagation. In the case of the spectroscopic luminosity, L, the uncertainty derives directly from the uncertainty on M_V (see Sect. 3) since the uncertainty on the bolometric correction BC is negligible. For the radius, R_*, the error propagates from the luminosity and temperature uncertainties. Luminosity, mass-loss and terminal velocity determine the uncertainty on the wind efficiency η. Finally the uncertainty on the ionizing fluxes, Q_0 and Q_1 derive directly from L, without taking into account internal model uncertainties.

Given the different nature of the two non-LTE codes, it is remarkable how similar the deduced parameters are. This confirms that despite the approximations adopted by ISA-WIND, this faster code is suitable for the analysis of Wolf-Rayet stars in the WC8 parameter domain (as it was also shown to be appropriate for a WN8 star by Crowther et al. 1999).

5.3. UV ionizing fluxes and bolometric luminosity

In Fig. 7 we present the predicted extreme UV fluxes from CMFGEN (solid line, top panel) and ISA-WIND (solid line, bottom panel) compared with the un-blanketed ISA-WIND model flux (dotted lines) on the energy vs log (λF_λ) plane.

As can be seen, the ISA-WIND flux at $\lambda \leq 400$ Å is harder than the CMFGEN flux, a discrepancy that was already pointed out by Crowther et al. (1999). On the other hand the Rydberg vs. λF_λ plot is designed to emphasise the 0–912 Å region

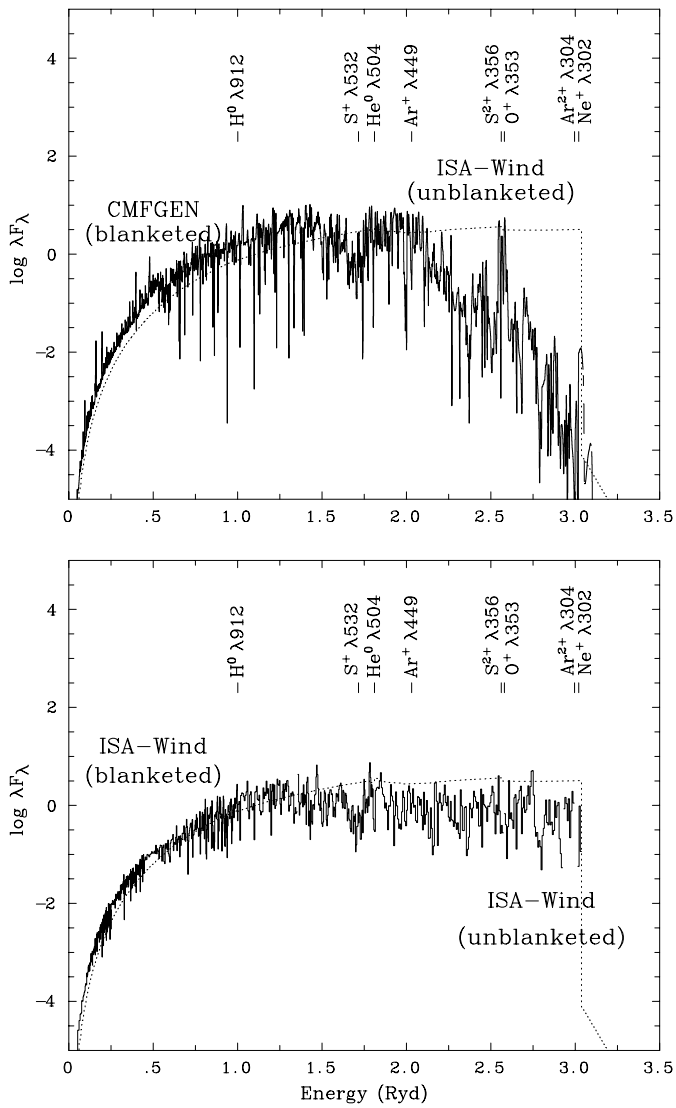

Fig. 7. Comparison between the output flux of CMFGEN (top) and ISA-wind (bottom). Both fluxes are compared to the un-blanketed ISA-WIND spectrum for the same stellar parameters

Table 3. Comparison of stellar parameters obtained for WR11 using CMFGEN and ISA-WIND (blanketed including photon loss)

Parameters	CMFGEN	ISA-wind	Error
Filling factor, f	10%	100%	
Photon Loss	–	yes	
T_* [kK]	57.1	56.0	3%
$\log(\dot{M}/\sqrt{f}\ [M_\odot\ \mathrm{yr}^{-1}])$	–4.53	–4.48	20%
C/He[by number]	0.15	0.06	40%
O/He[by number][a]	0.03	0.01	–
R [$R_\odot$]	3.2	3.2	20%
$\log(L_*/L_\odot)$	5.00	4.95	30%
BC [mag]	–4.00	–3.89	negl.
v_∞ [km s^{-1}]	1550	1550	10%
$\eta/\sqrt{f}$	21	28	60%
$\log(Q_0/\mathrm{s}^{-1})$	48.81	48.75	30%
$\log(Q_1/\mathrm{s}^{-1})$	47.76	47.83	30%

[a] This value follows from the adopted O/C=0.2

(1 Rydberg = 13.6 eV) and we see by looking at the values of $\log(Q_0/\mathrm{s}^{-1})$ and $\log(Q_1/\mathrm{s}^{-1})$ shown in Table 3, that in fact the two fluxes are not particularly dissimilar short of 912 Å and 504 Å. On the other hand, the fluxes shortward of $\sim$400 Å, which influence the strengths of nebular lines such as O^{2+}, Ar^{3+} and Ne^{2+}, are very different and this discrepancy could affect derived nebular properties.

The spectroscopic luminosity determined by CMFGEN and ISA-WIND are not dissimilar, although the former is slightly higher (Table 3). Both the luminosities are lower than that determined in Paper I from alternative methods ($\log(L/L_\odot)$ = 5.2$\pm$0.1), even considering the formal uncertainty determination.

The luminosity of 63000 $L_\odot$ obtained by Schaerer et al. (1997) can be compared to that obtained here by the CMFGEN code of 100 000 $L_\odot$. We can accredit the increase to the presence of line blanketing (which includes photon loss from the He II Lyα – see next section), although the difference of the two codes and the neglect of carbon and oxygen might also play a role.

6. The effect of line-line interaction

Line-line interaction between the very strong He II Lyα and nearby weaker lines has a large effect on the wind ionization structure. Approximations in the line-blanketing technique that affect either the position or the strength of even the weakest lines can affect greatly the derived stellar parameters. In this section we determine the size of this effect and show its consequences for the derived parameters of γ Velorum.

Schmutz (1997) proposed that capturing of He II Lyα line-photons by resonant metal transitions, would reduce the ionization balance of the wind. Including line-line interaction between He II Lyα and lines from ions such as Ca V, Fe VI, Ni VI and O III in his non-LTE model of the WN4 star WR6, led to a significantly lower wind ionization structure than that obtained without taking into account such interaction. As a result, he had to adopt a higher effective temperature to fit the spectrum of this star, leading to a larger luminosity and a lower wind performance number. In this way enough radiation force was obtained to drive the outer parts of the wind of WR6.

Schmutz (1997), however, carried out only an approximate calculation, which kept the fraction of photons captured by metal lines constant throughout the wind, instead of varying with radius. Additionally, the populations of the levels responsible for the metal transitions intercepting the He II photons, were calculated in LTE, instead of being calculated consistently with the populations of all other levels via the statistical equilibrium equations. Since the extent of this effect could lead to the long-sought answer to a driving mechanism for WR stars, we thought it important to investigate it further.

The line-blanketed CMFGEN code (Hillier & Miller 1999) automatically takes into account line-line interaction between all the lines included in the adopted atomic model so that photon loss should naturally take place in our calculation of Sect. 5, between He II Lyα and the included lines of iron, oxygen, calcium and carbon. To determine the effect of line-line interaction on the wind ionization, we removed from the atomic model, sets of lines in the spectral region neighboring ($\pm$2000 km s^{-1}) He II Lyα. *Throughout the rest of this discussion, we will refer to the model calculated with this reduced atomic model the "no-PL model" (which stands for no photon loss), while the model calculated in Sect. 5, which fits the spectrum of γ Velorum, is referred to as the "basic model"*.

The elimination of 21 Fe VI lines, results in a small increase in the wind ionization balance with respect to the model of Sect. 5. Next we eliminated the O III Bowen lines at 305.72 and 303.65 Å ($^3P -^3 P^o$ and $^3P -^3 D^o$) and a further increase in the ionization balance was observed. Next we eliminated 1 Ca V line, with no change in the calculated spectrum and finally we removed 63 C III lines, which produced a further small increase in the ionization balance. In Fig. 8 we compare the synthetic spectrum from the *basic model* (solid line) with the spectrum from the *no-PL model* (dashed line), while in Fig. 9 we present the corresponding ionization structures. The *basic model* presents a less ionized spectrum, with weaker He II lines and stronger He I lines. The ionization structure of helium is clearly higher in the *no-Pl model*, although that of carbon and oxygen appear similar, even if the lines of C IV follow the trend of the He II lines. Eliminating some metal lines does indeed change the wind ionization balance. The ionization structure and synthetic spectrum of the *basic model* can be matched if we increase the effective temperature of the *no-PL model* by about 10 000 K.

As a further test of the effect of line-line interaction on the overall wind ionization we calculated another model, with the same atomic data as in Sect. 5, but with the turbulent velocity of the lines in the He II Lyα ($\pm$300 km s^{-1}) region set at 5 km s^{-1}[2] instead of 50 km s^{-1}. In this way line-line interaction is reduced, since a smaller turbulent velocity leads to narrower lines, smaller overlap and therefore less interaction. *We refer to this model as the "low-vturb model"*

[2] This yields a Doppler velocity of 13 km s^{-1}.

Table 4. Summary of the stellar parameters obtained for WR11 using CMFGEN and ISA-WIND (blanketed with photon loss activated), compared with those derived by Schaerer et al. (1997) and De Marco et al. (1999a) with a non-line blanketed model with no photon loss implemented. The results obtained by Dessart et al. (2000) for WR135 are also included

Parameters	CMFGEN	ISA-wind	De Marco et al.	Schaerer et al.	WR135: Dessart et al.
Filling factor, f	10%	100%	100%	100%	10%
Photon Loss	–	yes	no	no	–
T_* (kK)	57.1	56.0	75.9	51.0	63.0
$\log(\dot{M}/\sqrt{f})$ $M_\odot$ yr^{-1}	–4.53	–4.48	–4.33	–4.2	–4.9
C/He (by number)	0.15	0.06	0.143	0.25	0.13
O/He (by number)	0.03	0.01	–	–	0.03
R (R$_\odot$)	3.2	3.2	1.84	3.3	3.4
$\log(L_*/L_\odot)$	5.00	4.95	5.01	4.8	5.20
BC (mag)	–4.00	–3.89	–4.1	–3.5	–4.0
v_∞ (km s^{-1})	1550	1550	1300	1450	1400
$\eta/\sqrt{f}$	21	28	29	144	5.4

In Fig. 8 we show the synthetic spectrum for the *low-vturb model* (dotted) compared to the *basic model* (solid), and the *no-PL model* (dashed), while in Fig. 9 we compare their respective ionization structures. The ionization equilibrium of the *low-vturb model* is higher than for the *basic model* but similar to the *no-PL model*. By reducing the line widths we have reduced the interaction between lines with an overall shift to a higher wind ionization, similar to the shift produced by the elimination of metal lines near He II Lyα.

The interception of continuum photons by metal lines (continuum blanketing) is an important effect and the shift in ionization observed when eliminating metal lines (solid and dashed lines in Figs. 8 and 9) *could* also be due to the lack of continuum blanketing by the lines we eliminated. The change in ionization between the *basic model* and the *low-vturb model* (solid and dotted lines in Figs. 8 and 9), on the other hand, is due to a reduced line-line interaction. The similarity of the ionization shifts in the two trials (dashed and dotted lines in Figs. 8 and 9), indicates that line-line interaction plays an important role in the change observed when eliminating metal lines. Weak but numerous metal lines, with wavelengths near that of strong emission lines are important in the overall ionization balance of the wind and therefore in the derived parameters.

From earlier trials we can estimate that the difference between the *basic model* (solid) and the *no-PL* or the *low-vturb* models (dashed and dotted, respectively) in Fig. 8 is equivalent to about 10 kK in effective temperature, but only about 20% in bolometric luminosity (because the radius to which the stellar temperature refers also changes). We can therefore conclude that *for this parameter space* photon-loss from the He II Lyα, does lead to a higher luminosity, although not as high as that determined via the evolutionary mass-luminosity relation.

7. Discussion

In the following sections we present a critical summary of the work carried out in this paper.

7.1. Stellar parameters and bolometric luminosity

We have presented a detailed spectroscopic analysis of the WR star in the γ Velorum WR+O binary system. Using the wavelength-dependent light ratio and the synthetic O star spectrum from Paper I we have generated a corrected WR optical and IR spectrum which we have fitted with a synthetic spectrum using the CMFGEN non-LTE model atmosphere code. Results are summarised in Table 4. Our derived mass-loss is in excellent agreement with the mass-loss derived by Stevens et al. (1996) from X-ray ASCA observations, once their value is scaled to the HIPPARCOS distance. Although the parameters of temperature, mass-loss and carbon abundance are well constrained, the oxygen abundance is assumed. The discrepancy between the He II lines at 4340, 4859 and 6560 Å and other He II lines remains to be explained.

Previous analyses of WR11 were carried out by Schaerer et al. (1997) and by De Marco et al. (1999a – using the stellar atmosphere code of Koesterke & Hamann, 1995). Schaerer et al. determined the stellar effective temperature by fitting the He I λ4471 / He II λ4541 ratio, assuming a (higher) mass-loss and carbon abundance. De Marco et al. (1999a) derived larger mass-loss and temperature, and a lower wind terminal velocity. This can be attributed to the fact that in the parameter space of γ Velorum the helium spectrum can be reproduced *approximately* with a range of temperature and mass-losses. On the other hand, when the lines are analysed in detail, it is clear that for temperatures larger than about 57 kK and $\log(\dot{M}/\mathrm{M}_\odot\ \mathrm{yr}^{-1})>-4.45$, predicted line shapes deteriorate, becoming wider. This effect was partly compensated for by De Marco et al. (1999a) by adopting a lower wind velocity, although it is clear from their fits that most lines are still too wide. Further, their neglect of line-blanketing and therefore of photon loss (no line-line interaction between the key lines), might have contributed to the different parameters.

With respect to the analysis of Schaerer et al. (1997), the star becomes twice as luminous, 10% hotter and shows a mass-loss lower by a factor of two. The carbon abundance is lower by 40% (although we remind the reader that Schaerer et al. *assumed* both the mass-loss and the carbon abundance). This carries implications for studies of wind-wind interaction. From

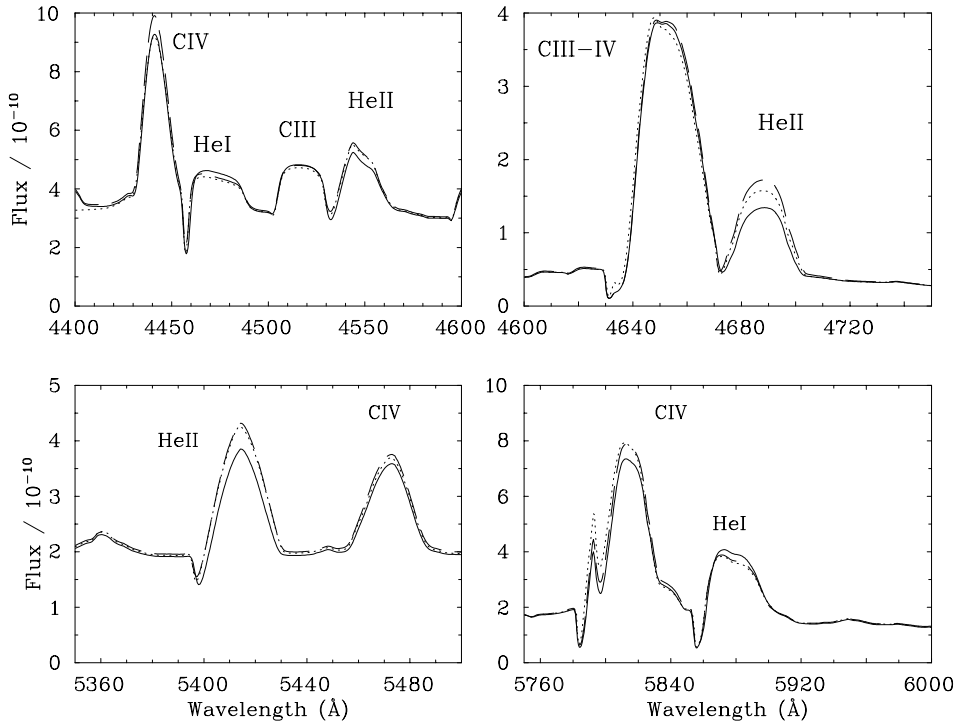

Fig. 8. Comparison between the model presented in Sect. 5 (solid), the model with metal lines in the He II Lyα region removed (dashed) and the model with the reduced $v_{\rm turb}$ (dotted)

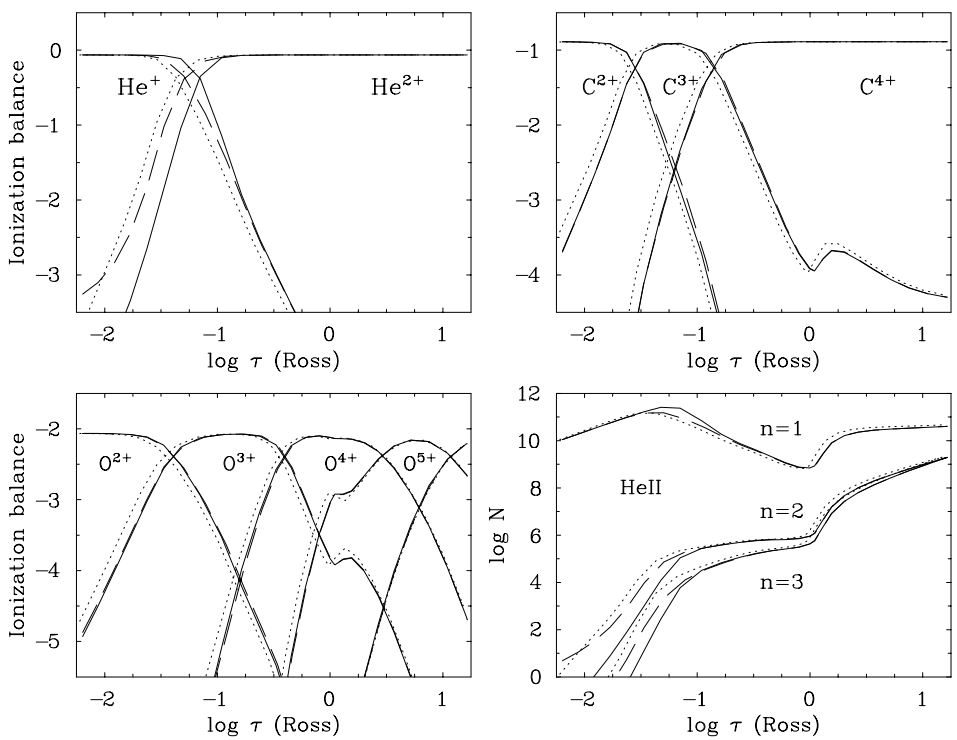

Fig. 9. Comparison between the ionization structure of helium, carbon, oxygen and the level population of He II for the models presented in Sect. 5 (solid), the model with metal lines in the He II Lyα region removed (dashed) and the model with the reduced v_{turb} (dotted)

this study and the results presented in Paper I for the O star, we determine:

$$\frac{(\dot{M}\, v_\infty)_{WR}}{(\dot{M}\, v_\infty)_O} \simeq 33$$

compared to a value of 208 derived by Schaerer et al. (1997). Adopting the relationships of Eichler & Usov (1993) we determine that the region of stellar wind collision is approximately 9–30 $R_\odot$ from the O star (0.15 of the distance that separates the two stars (63–200 $R_\odot$ – Schmutz et al. 1997) vs. 0.06 for the study of Schaerer et al. (1997)). Overall the stellar parameters derived are not dissimilar from those derived for the single WC8 star WR135 by Dessart et al. (2000; see Table 4). This indicates that it is unlikely that substantial levels of emission are produced by the collision region or that an anomalous ionization is induced by the O star ionizing flux.

The derived spectroscopic luminosity ($\log L/L_\odot = 5.0 \pm 0.1$) is increased with respect to that found in previous studies, partly due to line-line interaction, and is close to the luminosity derived in Paper I via the mass-luminosity relationship for WR stars ($\log L/L_\odot = 5.2 \pm 0.1$). An important implication of the higher luminosity and of a 10% clumping factor, is that it helps to reduce the performance number by a factor of ∼20, from 144 to 7, assuming a 10% clumping filling factor. Lucy & Abbott (1993) showed that radiation pressure on spectral lines should in principle be able to drive winds with performance numbers $\simeq 10$. So, the strongly reduced η suggests that line driving is the mechanism responsible for the dense wind of Wolf-Rayet component in γ Velorum.

7.2. CMFGEN *vs.* ISA-WIND

Parameters derived with the fast Sobolev approximation code ISA-WIND are similar to those derived with CMFGEN, apart from the derived carbon mass fraction, with CMFGEN resulting in a carbon abundance which is a factor of two larger than ISA-WIND. This discrepancy is not totally understood although we should note that the co-moving frame code of Koesterke & Hamann (1995) compares favourably with CMFGEN for cases in common (e.g. for WR135 – Dessart et al. 2000).

A secondary difference is in the fluxes at λ<400 Å. Crowther et al. (1999) tested the far UV model fluxes of CMFGEN and ISA-WIND by modelling the H II region associated with the WN8 star WR124, showing that, for that system, the ISA-WIND flux was too hard. Also in the current analysis we find that the ISA-WIND flux is harder for λ<400 Å: we suspect that this discrepancy is due to the lack of photon branching in the Monte Carlo code, which would lead to distributing energetic photons to longer wavelengths. Although the ionising properties of the two synthetic atmospheres (the values of Q_0 and Q_1) are similar, the difference in the extreme UV can carry implications when model WR fluxes are used to interpret nebular line emission from extra-galactic stellar populations (Leitherer et al. 1999).

We stress that the comparison between the two codes is reasonable only if photon loss is included in ISA-WIND via the approximation detailed in Sect. 4.3. If photon loss were not accounted for, the determined ISA-WIND effective temperature would be about 8000 K lower, comparable to the difference found in Sect. 6 when reducing the interaction between metal lines and He IILyα.

7.3. *The photon loss effect*

The photon loss effect demonstrated by Schmutz (1997) as the cause of a lower wind ionization, was tested here using the CMFGEN code which treats line-line interaction as part of the blanketing. For this parameter space the interaction between the He II Lyα and nearby O III and C III lines causes a shift to lower ionization equilibrium, equivalent to ∼10 000 K or a ∼20% increase in the luminosity[3]. By reducing the turbulent velocity from 50 to 5 km s^{-1} for lines residing near 303 Å, we have shown that the wind ionization is enhanced in a similar way, demonstrating that line-line interaction, and not continuum blanketing, is at the origin of the ionization shift observed when eliminating metal lines near the He II Lyα. If line-line interaction between strong resonance lines and weaker but more numerous metal lines leads to a shift in the wind ionization, a detailed treatment of even the weakest lines is important. We remind the reader that our test remains incomplete because, although CMFGEN treats line-line interaction not all lines are accounted for. Amongst the ones that are *not* treated there might be some that could play an important role in this mechanism. Additionally, our conclusion is only valid within the parameter space appropriate for WR11, a WC8 star, since for different temperature and mass-loss the strength of the He II and other strong lines will be different (cf. Crowther et al. (1999) who found that photon-loss did not play a role in the atmosphere of their WN8 star).

One should conclude from the presence of the photon loss mechanism that a proper treatment of the metal lines not only requires one to include very many lines (to realistically model the blanketing), but also the very critical ones, such as those near the strong He II Lyα and possibly at other resonance lines such as C IV at 1550 Å. Furthermore, the presence of photon loss shows that applying mean blanketing factors (Pauldrach et al. 1996) – averaged over 20–50 Å intervals – may miss out some interaction with an overall effect on the derived stellar parameters for WR stars. Finally, it is clearly pointed out that macro-turbulence is connected with photon loss, as the amount of turbulence essentially dictates the size and strength of the set of lines involved in the line-line interactions.

Acknowledgements. OD acknowledges support from PPARC grant PPA/G/S/1997/00780. PAC is funded by a Royal Society University Research Fellowship. DJH acknowledges support from NASA grants NAG5-8211 and NAGW-3828. AdK acknowledges support from NWO Pionier grant 600-78-333 to L.B.F.M. Waters and from NWO Spinoza grant 08-0 to E.P.J. van den Heuvel. JS acknowledges the grant Wo 296/22-1,3 by the Deutsche Forschungsgemeinschaft. Thanks to Patrick Morris and Karel van der Hucht for providing the ISO data, which is an ESA project with instruments funded by ESA member states (especially the PI countries: France, Germany, The Netherlands and the United Kingdom) with the partecipation of ISAS and NASA.

References

Anderson L.S., 1989, ApJ 339, 558
Castor J.I., 1970, MNRAS 149, 111
Crowther P.A., De Marco O., Barlow M.J., 1998, MNRAS 296, 367

[3] The quantification of the luminosity shift resulting from a different temperature depends on the location of the R_*, since this can change from model to model, it is not possible to simply derive the change in luminosity from the change in temperature and the Boltzman relationship.

Crowther P.A., Pasquali A., De Marco O., Schmutz W., de Koter A., 1999, A&A 350, 1007
Cousins A.W.J., 1972, Mon. Not. Astron. Soc. South Africa 31, 69
de Graauw T., Haser L.N., Beintema D.A., et al., 1996, A&A 315, 49
de Koter A., Schmutz W., Lamers H.J.G.L.M., 1993, A&A 277, 51
de Koter A., Heap S.R., Hubeny I., 1997, A&A 477, 792
De Marco O., Schmutz W., 1999, A&A 345, 163
De Marco O., Schmutz W., Koesterke L., Hamann W.-R., de Koter A., 1999a, In: van der Hucht K.A., Koenisberger G., Eenens P.R.J. (eds.) Wolf-Rayet Phenomena in Massive Stars and Starburst Galaxies. Proc. IAU Symp. 193, ASP, p. 227
De Marco O., Schmutz W., Koesterke L., Hamann W.-R., 1999b, In: van der Hucht K.A., Koenisberger G., Eenens P.R.J. (eds.) Wolf-Rayet Phenomena in Massive Stars and Starburst Galaxies. Proc. IAU Symp. 193, ASP, p. 231
Dessart L., Crowther P.A., Hillier D.J., et al., 2000, MNRAS, in press (astro-ph/0001228)
Eicher D., Usov V., 1993, ApJ 402, 271
Hillier D.J., 1987, ApJS 63, 947
Hillier D.J., 1989, ApJ 347, 329
Hillier D.J., 1990, A&A 231, 116
Hillier D.J., Miller D.L., 1998, ApJ 496, 407
Hillier D.J., Miller D.L., 1999, ApJ 519, 354
Johnson H.L., Iriarte B., Mitchell R.I., Wisniewski W.Z., 1966, Comm. Lunar Plan. Lab. 4, 99
Kessler M.F., Steinz J.A., Anderegg M.A., et al., 1996, A&A 315, L27
Koesterke L., Hamann W.-R., 1995, A&A 299, 503
Leitherer C., Schaerer D., Goldader J.D., et al., 1999, ApJS 123, 3
Lucy L.B., Abbott D.C., 1993, ApJ 405, 738
Meynet G., Maeder A., Schaller G., Schaerer D., Charbonnel C., 1994, A&AS 103, 97
Moffat A.F.J., 1999, In: van der Hucht K.A., Koenigsberger G., Eenens P.R.J. (eds.) Wolf-Rayet Phenomena in Massive Stars and Starburst Galaxies. Proc. IAU Symp. No. 193, ASP, San Francisco, p. 278
Morris P.W., van der Hucht K.A., Crowther P.A., et al., 2000, A&A 353, 624
Pauldrach A.W.A., Duschinger M., Mazzali P.A., et al., 1996, A&A 312, 525
Pozzo M., Jeries R.D., Naylor T., et al., 2000, MNRAS 313, L23
Schaerer D., Maeder A., 1992, A&A 263, 129
Schaerer D., Schmutz W., Grenon M., 1997, ApJ 484, L153
Schmutz W., 1991, In: Crivellary L., Hubeny I., Hummer D.G. (eds.) Stellar Atmospheres: Beyond Classical Models. NATO ASI Ser. C Vol. 341, Kluwer, Dordrecht, p. 191
Schmutz W., 1995. In: van der Hucht K.A., Williams P.M. (eds.) Proc. IAU Symp. 163, Wolf-Rayet Stars: Binaries, Colliding Winds, Evolution. Kluwer, Dordrecht, p. 127
Schmutz W., 1997, A&A 321, 268
Schmutz W., Vacca W.D., 1991, A&AS 89, 259
Schmutz W., Schweickhardt J., Stahl O., et al., 1997, A&A 328, 219
Seaton M.J., 1979, MNRAS 187, 73
Smith L.F., 1968, MNRAS 140, 409
Stevens I.R., Corcoran M.F., Willis A.J., et al., 1996, MNRAS 283, 589
St-Louis N., Willis A.J., Stevens I.R., 1993, ApJ 415, 298
Turner D.G., 1982, In: de Loore C.W.H., Willis A.J. (eds.) Wolf-Rayet Stars: Observations, Physics, Evolution. Proc. IAU Symp. 99 Reidel, Dordrecht, p. 57
van der Hucht K.A., Hidayat B., Admiranto A.G., Supelli K.R., Doom C., 1988, A&A 199, 217
Willis A.J., Wilson R., 1976, A&A 47, 429